JACS
JOURNAL OF THE AMERICAN CHEMICAL SOCIETY

Communication

pubs.acs.org/JACS

Solution NMR Experiment for Measurement of $^{15}N-^{1}H$ Residual Dipolar Couplings in Large Proteins and Supramolecular Complexes

Alexander Eletsky,[†] Surya V.S.R.K. Pulavarti,[†] Victor Beaumont,[†,§] Paul Gollnick,[‡] and Thomas Szyperski*[,†]

[†]Department of Chemistry and [‡]Department of Biological Sciences, State University of New York at Buffalo, Buffalo, New York 14260, United States

Supporting Information

ABSTRACT: NMR residual dipolar couplings (RDCs) are exquisite probes of protein structure and dynamics. A new solution NMR experiment named 2D SE2 *J*-TROSY is presented to measure N−H RDCs for proteins and supramolecular complexes in excess of 200 kDa. This enables validation and refinement of their X-ray crystal and solution NMR structures and the characterization of structural and dynamic changes occurring upon complex formation. Accurate N−H RDCs were measured at 750 MHz ^{1}H resonance frequency for 11-mer 93 kDa $^{2}H,^{15}N$-labeled Trp RNA-binding attenuator protein tumbling with a correlation time τ_c of 120 ns. This is about twice as long as that for the most slowly tumbling system, for which N−H RDCs could be measured, so far, and corresponds to molecular weights of ∼200 kDa at 25 °C. Furthermore, due to the robustness of SE2 *J*-TROSY with respect to residual ^{1}H density from exchangeable protons, increased sensitivity at ^{1}H resonance frequencies around 1 GHz promises to enable N−H RDC measurement for even larger systems.

Nuclear magnetic resonance (NMR) studies of large proteins and supramolecular complexes (≫∼100 kDa) rely on transverse relaxation optimized spectroscopy[1] (TROSY) with samples having backbone $^{15}N^{1}H$ and/or side chain $^{13}C^{1}H_3$ moieties in a uniformly ^{2}H-labeled background. Strategies for respective $^{15}N,^{13}C,^{1}H$ resonance assignment exist,[2] and structural constraints can be derived from backbone chemical shifts,[3] $^{1}H-^{1}H$ nuclear Overhauser effects, and paramagnetic relaxation enhancement, potentially combined with constraints from "evolutionary coupling" of sequence variations.[4] N−H residual dipolar coupling (RDC)[5] measurements are thus far restricted to τ_c < ∼50−60 ns because an experiment to readily measure N−H RDCs for very large systems is not available (Supporting Information, Figure S1). Here we present a solution NMR experiment to measure such RDCs for systems tumbling with τ_c well above 100 ns.

For $\tau_c \gg 50$ ns, the major limitation for N−H RDC (*D*-coupling) measurement arises from very fast relaxation of the ^{15}N "anti-TROSY" transition[6] during scalar coupling (*J*) evolution. Hence, any new approach needs to separate *J* evolution from TROSY-based ^{15}N frequency labeling. Sensitivity enhancement (SE) during a delay τ_J can then be achieved via simultaneous detection of both orthogonal signal components resulting from *J* evolution,[7] analogous to preservation of equivalent pathways.[8] Furthermore, it is highly advantageous if *J* evolution does not shift peak positions in 2D [$^{15}N,^{1}H$] spectra (as for frequency domain measurements[6,9]), so that peak assignments can be readily retained.

Based on these criteria, we implemented a novel TROSY-based experiment. As in constant time *J*-HSQC,[8b] *J* evolves during a fixed delay τ_J and is encoded in peak intensities in two subspectra recorded, respectively, with the radio frequency (rf) pulse modules (1) and (2) of Figure 1. In the absence of differential spin relaxation, addition (+) and subtraction (−) of the subspectra yields $\cos(\pi J\tau_J)$- and $\sin(\pi J\tau_J)$-scaled 2D [$^{15}N,^{1}H$] TROSY spectra; *J* is calculated from the peak volumes $V^{(+)}$ and $V^{(-)}$ as

$$J = \arctan(V^{(-)}/V^{(+)})/(\pi\tau_J) + n/\tau_J \quad (1)$$

if *J* evolution is *n*-fold aliased during τ_J (Supporting Information 2). Moreover, calculation of error propagation reveals that precision is highest at $\tau_J = 1/R_{2N}$, the inverse average transverse relaxation rate of ^{15}N in-phase and antiphase coherences (Supporting Information 3). Importantly, the ST2-PT TROSY pulse module[1b,10] allows combining pulse field gradient (PFG)-based SE during ^{15}N-shift evolution with the second SE during *J* evolution (product operator[11] calculation in Supporting Information 2). Hence, the new experiment is "doubly" sensitivity enhanced and named "2D SE2 *J*-TROSY" (for brevity, we will refer to 2D SE TROSY[1b,10] as 2D TROSY).

We compared the theoretically expected *precision* of *J* measurement of SE2 *J*-TROSY (Figure 1) with two other TROSY-based approaches, "amide RDCs by TROSY spectroscopy" (ARTSY)[13] and *J*-modulated TROSY, congener of *J*-modulated HSQC.[14] ARTSY is the most sensitive approach available thus far for large systems. It involves recording two 2D TROSY spectra acquired with *J* evolution of transverse $^{1}H^{N}$ magnetization during an initial INEPT delay extended to $\tau_A \approx 1/J$. For the first and second spectrum, *J* evolution effectively evolves, respectively, during τ_A and $\tau_A/2$. *J*-modulated TROSY relies on sampling $\cos(\pi J\tau)$ evolution at multiple delays τ prior to ^{15}N frequency labeling, requiring comparably long *J* evolution times for precise measurement of *J*.[14] The same holds for frequency-based methods such as 2D CE-TROSY[6,9b] and recording two 2D TROSY spectra with and without ^{1}H

Received: July 6, 2015
Published: August 21, 2015

DOI: 10.1021/jacs.5b07010
J. Am. Chem. Soc. 2015, 137, 11242−11245

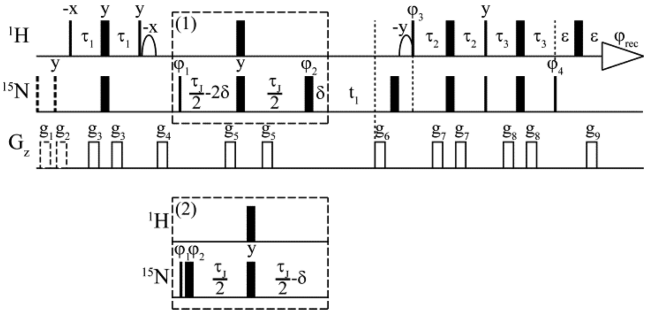

Figure 1. Radio frequency pulse sequence of 2D SE2 *J*-TROSY. Modules in dashed boxes labeled (1) and (2) are applied to acquire two subspectra. $\tau_J \approx 1/R_{2N}$ is the delay for *J* evolution. Rectangular 90 and 180° pulses are indicated by thin and thick vertical bars, and phases for Agilent spectrometers are indicated above the pulses. Where no rf phase is marked, the pulse is applied along *x*. $\delta = 2pwN/\pi$ compensates for shift and *J* evolution during the 90° ^{15}N rf pulse of duration *pwN* (phase φ_1) and subsequent 180° ^{15}N and ^{1}H rf pulses (Supporting Information 2). High-power 90° pulse lengths: ~13 μs for ^{1}H, ~34 μs for ^{15}N. Duration and strengths of sine-bell-shaped PFGs: G$_1$ (0.5 ms, 14.7 G/cm); G$_2$ (0.5 ms, 10.3 G/cm); G$_3$ (0.5 ms, −14.7 G/cm); G$_4$ (1 ms, 26.6 G/cm); G$_5$ (1 ms, 14.2 G/cm); G$_6$ (2 ms, 31.9 G/cm); G$_7$ (0.5 ms, 17 G/cm); G$_8$ (0.5 ms, 8 G/cm); G$_9$ (0.2 ms, 32.4 G/cm). τ_J, τ_1, τ_2, τ_3, and phase φ_4 (Table S1) are optimized for higher sensitivity and/or artifact suppression (Supporting Information 2.3). Phase cycling: $\varphi_1 = x, -x$; $\varphi_2 = x, x, y, y, -x, -x, -y, -y$; $\varphi_3 = x$; $\varphi_4 = y$; $\varphi_{rec} = x, -x, -x, x$. Quadrature detection in t_1(^{15}N): recording of a second data set with phases φ_3, φ_4, and gradient G$_9$ inverted.[10] Water magnetization is flipped back[12] by two 1.4 ms soft pulses (sinc center lobe). Dashed 90° ^{15}N pulses and gradients G$_1$ and G$_2$ purge ^{15}N steady-state magnetization to quantify the impact of ΔR on *J* measurement (see text); they should be omitted for somewhat improved sensitivity and accuracy of *J* measurement (Supporting Information 4). ^{15}N CSA/DD cross-correlated relaxation during τ_J is identical for modules (1) and (2) (except for 2δ, which is negligible).

decoupling in t_1(^{15}N).[15] For these two experiments, *J* evolution is cosine sampled in concert with ^{15}N frequency labeling, and intrinsic sensitivities are comparable to *J*-modulated TROSY. Hence, we focused on comparing SE2 TROSY with ARTSY and *J*-modulated TROSY.

We performed error propagation calculations (Figure 2) for a rigid, isotropically reorienting ^{2}H,^{15}N-labeled protein neglecting differential relaxation of in-phase/antiphase terms as well as ^{15}N chemical shift anisotropy (CSA)/^{15}N−^{1}H dipole−dipole (DD) cross-correlated relaxation during *J* evolution (Supporting Information 3). Figure 2 shows that (i) for τ_c up to ~30 ns, all three experiments promise to yield, for both β-sheets and α-helices, comparable precision; (ii) for τ_c > ~30 ns, *J*-modulated TROSY is significantly less precise than SE2 TROSY and ARTSY; (iii) for τ_c > ~75 ns, ARTSY is expected to be significantly less precise than SE2 *J*-TROSY for α-helices (due to the higher residual ^{1}H density when compared with β-sheets); and (iv) for τ_c > ~120 ns, ARTSY is less precise than SE2 *J*-TROSY also for β-sheets. Importantly, even for τ_c > ~120 ns, SE2 *J*-TROSY is expected to yield quite similar precision for α-helices and β-sheets, reflecting its robustness with respect to residual ^{1}H density. This is because sensitivity of SE2 *J*-TROSY depends on R_{2N} (during *J* evolution), which is affected to a lesser degree by the residual proton density than R_{2H} (during *J* evolution) as in ARTSY.

We then assessed the theoretical *accuracy* of *J* measurement with SE2 *J*-TROSY. Accuracy is reduced by spin relaxation during τ_J affecting $V^{(-)}/V^{(+)}$, that is, differential relaxation of $N^{\pm}$

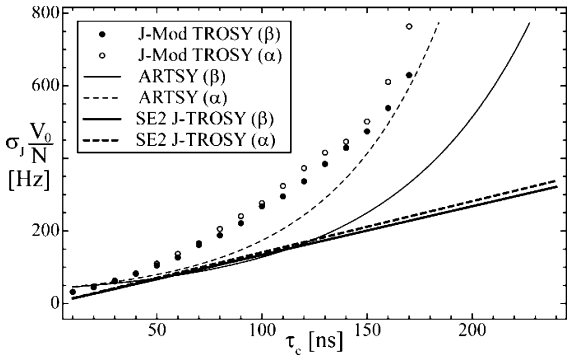

Figure 2. Precision of *J* measurement calculated for a ^{15}N,^{2}H-labeled protein tumbling at τ_c: SE2 *J*-TROSY (thick lines), ARTSY (thin lines), and *J*-modulated TROSY (dots) ^{1}H^N−^{1}H^N distances in secondary structure elements and 3.4% residual protonation were considered (Supporting Information 5). Plotted versus τ_c is the product of the standard deviations for *J* measurement, σ_J, and the "volume over noise ratio", V_0/N, observed in a reference TROSY spectrum. The curves for SE2 *J*-TROSY and ARTSY are from analytical solutions of error propagation calculations, and dots for *J*-modulated TROSY are from simulations (Supporting Information 3).

and $2N^{\pm}H_z$,[16] and CSA/DD cross-correlated relaxation resulting in differential relaxation of $N^{\pm}H^{\beta}$ and $N^{\pm}H^{\alpha}$. Hence, we followed previous studies[16a,17] to solve the Liouville−von Neumann equation for the 4D subspace spanned by N_y, $2N_xH_z$, N_x, and $2N_yH_z$, considering rf pulses (Figure 1), chemical shift, and *J* evolution during τ_J for the spin Hamiltonian. In contrast to the previous studies, we derived an analytical solution considering both the difference of $N^{\pm}$ and $2N^{\pm}H_z$ relaxation rates,[16b] ΔR, and the ^{15}N CSA/DD cross-correlated relaxation rate η_N in the regime $(\Delta R/(2\pi J))^2 \ll 1$ and $(\Delta R/(2\eta_N))^2 \ll 1$ (Supporting Information 4). For large τ_c, relaxation significantly affects the measured coupling, J_{app}, obtained with eq 1. Although $V^{(-)} \sim \sin(\pi J\tau_J)$ still holds, one finds, as eq 2

$$V^{(+)} \propto \cos(\pi J\tau_J) + \frac{\Delta R(\eta_N(\exp(-\eta_N\tau_J) - \cos(\pi J\tau_J)) - \pi J\sin(\pi J\tau_J))}{2(\eta_N^2 + (\pi J)^2)} \quad (2)$$

Figure 3a shows $\Delta J = (J_{app} - J)$ versus τ_c, where ΔJ was calculated using eq S81 (Supporting Information 5) for a rigid ^{2}H,^{15}N-labeled protein tumbling isotropically (J = −93 Hz; 750 MHz). Up to $\tau_c \sim$ 70 ns, $\Delta J/J$ < 1%, so that SE2 *J*-TROSY enables accurate measurement, while $\Delta J/J$ becomes significant for large τ_c and reaches, respectively, ~5 and ~12% for β-sheets and α-helices at $\tau_c \sim$ 200 ns. Since ΔR and η_N are difficult to measure accurately for large systems, extraction of *J* from J_{app} values is challenging for τ_c > ~70 ns. However, *D* is obtained from the difference of couplings with and without partial alignment: $D_{app} = (J + D)_{app} - J_{app}$. Since τ_c is very similar with and without alignment,[18] $\Delta(J + D)$ and ΔJ cancel largely. Figure 3b shows $\Delta D = \Delta D_{app} - \Delta J_{app}$ for J = −93 Hz in α-helices, where ΔR is larger than that in β-sheets (Figure 3a), for $\tau_c \sim$ 120 ns and *D* varying between −20 and +10 Hz. The calculations predict that *D* can be accurately measured (within ~1 Hz) for $\tau_c \sim$ 120 ns. Furthermore, $\Delta(J + D)$ is approximately proportional to $J + D$, so that ΔD is proportional to *D*. For uniform ΔR and η_N values, such a systematic error with $\Delta D \sim D$ solely yields a change of the apparent magnitude of the alignment tensor but not inaccurate orientational constraints. Finally, differential

DOI: 10.1021/jacs.5b07010
J. Am. Chem. Soc. 2015, 137, 11242−11245

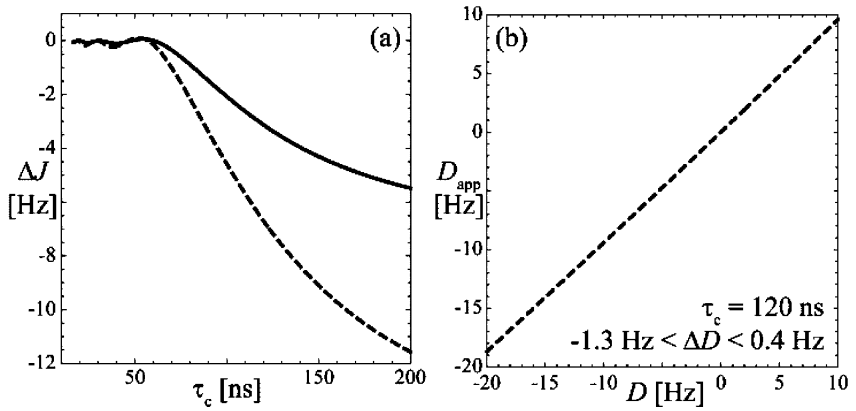

Figure 3. (a) Plot of calculated $\Delta J = (J_{app} - J)$ versus τ_c at $\tau_J = 1/R_{2N}$ for a rigid $^2H,^{15}N$-labeled protein tumbling isotropically ($J = -93$ Hz; 750 MHz); the distances between $^1H^N$ and other ^1H are as in Figure 2 (solid line, β-sheet; dashed line, α-helix). (b) For α-helix at $\tau_c = 120$ ns: plot of $D_{app} = (J + D)_{app} - J_{app}$ versus D between −20 and +10 Hz. The corresponding range of ΔD is indicated at the bottom; small ΔD allows derivation of orientational constraints.[5]

dynamic frequency shifts for $N^{\pm}H^{\beta}$ and $N^{\pm}H^{\alpha}$[14,19] have been shown to be only ∼0.7 Hz for $\tau_c >$ ∼10 ns,[19] and they cancel likewise.

We verified experimentally high precision and accuracy of J measurement with SE2 J-TROSY for a ∼1 mM solution of 16 kDa protein "OR457" (τ_c ∼ 8 ns; PDB ID 2MR5) without and with partial Pf1 phage[18] alignment. We acquired in duplicate SE2 J-TROSY as well as J-modulated HSQC spectra.[14] This yielded a rmsd of ∼0.2 Hz calculated between duplicate sets of D-couplings with either of the two methods and ∼0.6 Hz between sets obtained with the two methods (Supporting Information 10).

Next, we acquired (Supporting Information 9) in duplicate (i) SE2 J-TROSY, ARTSY, and J-modulated TROSY data at 750 MHz and 47.5 °C for a ∼0.22 mM solution of tryptophan-bound 11-mer 93 kDa $^2H,^{15}N$-labeled Trp RNA-binding attenuator protein (TRAP) from *B. stearothermophilus*[20] (τ_c ∼ 31 ns; Supporting Information 8) without and with Pf1 phage alignment (Figure 4), and (ii) SE2 J-TROSY and ARTSY data at 0 °C (τ_c ∼ 120 ns; Figure 5). $^{15}N/^1H$ assignments at 47.5 °C[21] were confirmed using 3D ^{15}N-resolved $[^1H-^1H]$ NOESY and transferred to 0 °C with a 2D TROSY temperature series. All chemical shifts changed according to temperature coefficients expected for a folded protein,[22] confirming that TRAP does not

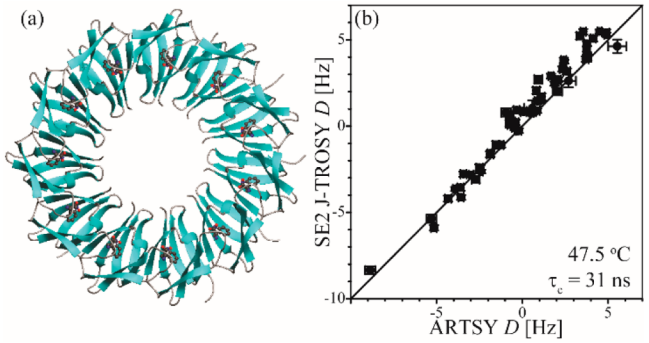

Figure 4. (a) Ribbon drawing of 93 kDa 11-mer TRAP from *B. stearothermophilus*[20] with Trp (shown as "ball-and-stick" representations) bound to the subunits (PDB ID: 1QAW). (b) D-couplings and standard deviations (calculated via error propagation from peak V/N ratios; bars) measured at 47.5 °C (τ_c ∼ 31 ns; measurement time 47 h for each experiment; V_0/N ∼ 270 in reference 2D TROSY; Table S1).

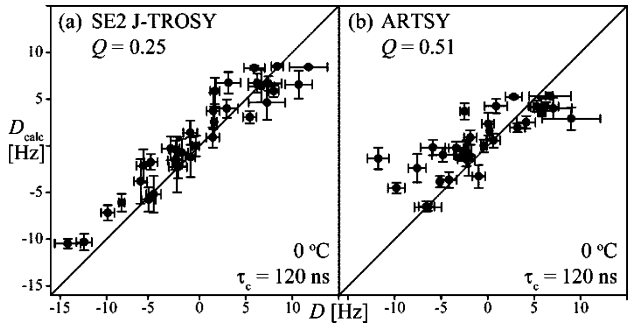

Figure 5. D_{calc} predicted from TRAP structure versus D measured at 0 °C (τ_c ∼ 120 ns) with (a) SE2 J-TROSY and (b) ARTSY. For D, the mean of the duplicate measurements (Table S1) and standard deviations (calculated via error propagation from peak V/N ratios; horizontals bars) are displayed. For D_{calc}, mean values and standard deviations (vertical bars) are displayed as obtained for the 11 subunits of the TRAP X-ray crystal structure (total measurement time 84 h for each experiment; V_0/N ∼ 180 in reference TROSY; Table S1).

(partially) cold denature. Consistently, τ_c values measured (Supporting Information 10) at 0 °C (∼120 ns) and 47.5 °C (31 ns) are in close agreement with hydrodynamic calculations (120 and 32 ns, respectively; Supporting Information 7) for the TRAP structure[20] (Figure 4a). The structure was also used to calculate Q-factors to assess agreement with D-couplings.

At 47.5 °C (τ_c ∼ 31 ns; Figure 4; Supporting Information 10), the same high precision of J and D measurement was obtained, as predicted (Figure 2), for SE2 J-TROSY (rmsd values between duplicate sets of 58 J- and D-couplings from well-resolved peaks are 0.28 and 0.39 Hz), ARTSY (0.33 and 0.43 Hz), and J-modulated TROSY (0.37 and 0.50 Hz). High accuracy of D measurement was validated with (i) rmsd values for sets of D-couplings from SE2 J-TROSY versus ARTSY (0.81 Hz, Figure 4b), SE2 J-TROSY versus J-modulated TROSY (0.96 Hz), ARTSY versus J-modulated TROSY (0.62 Hz); and (ii) low Q-factors of 0.22, 0.23, and 0.20 obtained, respectively, for D-couplings from SE2 J-TROSY, ARTSY, and J-modulated TROSY.

In accordance with predictions (Figure 2), at 0 °C (τ_c ∼ 120 ns), J-modulated TROSY is not sufficiently sensitive, while rather *precise* RDCs are obtained (Supporting Information 10) with SE2 J-TROSY (rmsd between duplicate sets of 45 RDCs is 1.9 Hz) and ARTSY (2.3 Hz). However, Q-factors (SE2 J-TROSY =

DOI: 10.1021/jacs.5b07010
J. Am. Chem. Soc. 2015, 137, 11242−11245

0.25; ARTSY = 0.51) (Figure 5; Supporting Information 10) revealed that only SE2 *J*-TROSY offered sufficient *accuracy* to derive orientational constraints (rmsd between SE2 and ARTSY derived RDC sets = 3.0 Hz). This finding may, at least partially, be due to the fact that ARTSY is affected to a larger degree by $^{1}H^{N}$ CSA/DD cross-correlated relaxation than SE2 *J*-TROSY is by ΔR and ^{15}N CSA/DD relaxation ($^{1}H^{N}$ cross-correlated relaxation is only partially suppressed in the second ARTSY spectrum[13]).

We showed that SE2 *J*-TROSY employed at a moderately high ^{1}H frequency of 750 MHz enables accurate measurement of N−H RDCs up to $\tau_c \sim 120$ ns, which corresponds to molecular weights of ∼200 kDa at 25 °C. Moreover, increased sensitivity offered by 1.0−1.2 GHz spectrometers close to the "magic TROSY field",[1a] along with sensitivity enhancement from paramagnetic relaxation agents[23] and possibly dynamic nuclear polarization,[24] promises to enable N−H RDC measurement up to $\tau_c \sim 200$ ns. For even longer τ_c, residual ^{1}H density can be reduced by adding 50% $^{2}H_2O$, and cross-relaxation-induced polarization transfer[25] can be employed. Notably, (i) solid-state NMR spectroscopy promises to enable sequential N−H resonance assignment for even the largest systems,[26] and (ii) aromatic TROSY-based[27] SE2 *J*-TROSY can be envisaged for aromatic $^{13}C-^{1}H$ RDCs[28] with alternate ^{13}C labeling.[29]

SE2 *J*-TROSY measurement of N−H RDCs will enable (i) assessment and refinement of X-ray structures of large proteins and supramolecular complexes for solution studies, (ii) structure-based $^{15}N/^{1}H$ resonance assignment, and (iii) characterization of conformational and dynamic changes upon complex formation (e.g., to study allostery). The new approach alleviates an important size limitation of solution NMR.

■ ASSOCIATED CONTENT

Supporting Information

The Supporting Information is available free of charge on the ACS Publications website at DOI: 10.1021/jacs.5b07010.

Details of sample preparation, methods, and results (PDF)

■ AUTHOR INFORMATION

Corresponding Author

*szypersk@buffalo.edu

Present Address

§(V.B.) Department of Chemistry, Yale University, New Haven, Connecticut 06520, United States.

Notes

The authors declare no competing financial interest.

■ ACKNOWLEDGMENTS

This work was supported by the NSF (MCB 0817857 to T.S. and MCB 1019969 to P.G.) and NIH (U54 GM094597 to T.S.). We thank Dr. M. Foster, Ohio State University, for providing TRAP backbone $^{15}N/^{1}H$ chemical shifts and for recommending alignment with Pf1 phages, and Drs. A. Ghosh and B. Sathyamoorthy for support in the initial phase of the project.

■ REFERENCES

(1) (a) Pervushin, K.; Riek, R.; Wider, G.; Wuthrich, K. *Proc. Natl. Acad. Sci. U. S. A.* **1997**, *94*, 12366−12371. (b) Pervushin, K. V.; Wider, G.; Wuthrich, K. *J. Biomol. NMR* **1998**, *12*, 345−348. (c) Tugarinov, V.; Hwang, P. M.; Ollerenshaw, J. E.; Kay, L. E. *J. Am. Chem. Soc.* **2003**, *125*, 10420−10428.

(2) Goebl, C.; Madl, T.; Simon, B.; Sattler, M. *Prog. Nucl. Magn. Reson. Spectrosc.* **2014**, *80*, 26−63.

(3) Shen, Y.; Lange, O.; Delaglio, F.; Rossi, P.; Aramini, J. M.; Liu, G.; Eletsky, A.; Wu, Y.; Singarapu, K. K.; Lemak, A.; Ignatchenko, A.; Arrowsmith, C. H.; Szyperski, T.; Montelione, G. T.; Baker, D.; Bax, A. *Proc. Natl. Acad. Sci. U. S. A.* **2008**, *105*, 4685−4690.

(4) Tang, Y.; Huang, Y. J.; Hopf, T. A.; Sander, C.; Marks, D. S.; Montelione, G. T. *Nat. Methods* **2015**, *12*, 751−754.

(5) (a) Chen, K.; Tjandra, N. The Use of Residual Dipolar Coupling in Studying Proteins by NMR. In *NMR of Proteins and Small Biomolecules*; Zhu, G., Ed.; Springer: Berlin, 2012; Vol. *326*, pp 47−67. (b) de Alba, E.; Tjandra, N. *Prog. Nucl. Magn. Reson. Spectrosc.* **2002**, *40*, 175−197. (c) Prestegard, J. H.; Bougault, C. M.; Kishore, A. I. *Chem. Rev.* **2004**, *104*, 3519−3540.

(6) Bhattacharya, A.; Revington, M.; Zuiderweg, E. R. P. *J. Magn. Reson.* **2010**, *203*, 11−28.

(7) Atreya, H. S.; Garcia, E.; Shen, Y.; Szyperski, T. *J. Am. Chem. Soc.* **2007**, *129*, 680−692.

(8) (a) Palmer, A. G.; Cavanagh, J.; Wright, P. E.; Rance, M. *J. Magn. Reson.* **1991**, *93*, 151−170. (b) Tolman, J. R.; Prestegard, J. H. *J. Magn. Reson., Ser. B* **1996**, *112*, 245−252.

(9) (a) Ding, K. Y.; Gronenborn, A. M. *J. Magn. Reson.* **2003**, *163*, 208−214. (b) Jain, N. U.; Noble, S.; Prestegard, J. H. *J. Mol. Biol.* **2003**, *328*, 451−462.

(10) Weigelt, J. *J. Am. Chem. Soc.* **1998**, *120*, 10778−10779.

(11) Sorensen, O. W.; Eich, G. W.; Levitt, M. H.; Bodenhausen, G.; Ernst, R. R. *Prog. Nucl. Magn. Reson. Spectrosc.* **1984**, *16*, 163−192.

(12) Grzesiek, S.; Bax, A. *J. Am. Chem. Soc.* **1993**, *115*, 12593−12594.

(13) Fitzkee, N. C.; Bax, A. *J. Biomol. NMR* **2010**, *48*, 65−70.

(14) Tjandra, N.; Grzesiek, S.; Bax, A. *J. Am. Chem. Soc.* **1996**, *118*, 6264−6272.

(15) Schwieters, C. D.; Suh, J.-Y.; Grishaev, A.; Ghirlando, R.; Takayama, Y.; Clore, G. M. *J. Am. Chem. Soc.* **2010**, *132*, 13026−13045.

(16) (a) Harbison, G. S. *J. Am. Chem. Soc.* **1993**, *115*, 3026−3027. (b) Peng, J. W.; Wagner, G. *Biochemistry* **1992**, *31*, 8571−8586.

(17) (a) Ghose, R.; Prestegard, J. H. *J. Magn. Reson.* **1998**, *134*, 308−314. (b) Meersmann, T.; Bodenhausen, G. *Chem. Phys. Lett.* **1996**, *257*, 374−380.

(18) Hansen, M. R.; Mueller, L.; Pardi, A. *Nat. Struct. Biol.* **1998**, *5*, 1065−1074.

(19) Bruschweiler, R. *Chem. Phys. Lett.* **1996**, *257*, 119−122.

(20) Chen, X. P.; Antson, A. A.; Yang, M.; Li, P.; Baumann, C.; Dodson, E. J.; Dodson, G. G.; Gollnick, P. *J. Mol. Biol.* **1999**, *289*, 1003−1016.

(21) McElroy, C.; Manfredo, A.; Wendt, A.; Gollnick, P.; Foster, M. *J. Mol. Biol.* **2002**, *323*, 463−473.

(22) Baxter, N. J.; Williamson, M. P. *J. Biomol. NMR* **1997**, *9*, 359−369.

(23) Oktaviani, N.; Risør, M.; Lee, Y.-H.; Megens, R.; de Jong, D.; Otten, R.; Scheek, R.; Enghild, J.; Nielsen, N.; Ikegami, T.; Mulder, F. A. *J. Biomol. NMR* **2015**, *62*, 129−142.

(24) Günther, U. L. Dynamic Nuclear Hyperpolarization in Liquids. In *Modern NMR Methodology*; Heise, H., Matthews, S., Eds.; Springer: Berlin, 2013; Vol. *335*, pp 23−69.

(25) Riek, R.; Wider, G.; Pervushin, K.; Wuthrich, K. *Proc. Natl. Acad. Sci. U. S. A.* **1999**, *96*, 4918−4923.

(26) Mainz, A.; Religa, T. L.; Sprangers, R.; Linser, R.; Kay, L. E.; Reif, B. *Angew. Chem., Int. Ed.* **2013**, *52*, 8746−8751.

(27) Eletsky, A.; Atreya, H. S.; Liu, G. H.; Szyperski, T. *J. Am. Chem. Soc.* **2005**, *127*, 14578−14579.

(28) Sathyamoorthy, B.; Singarapu, K. K.; Garcia, A. E.; Szyperski, T. *ChemBioChem* **2013**, *14*, 684−688.

(29) (a) Milbradt, A. G.; Arthanari, H.; Takeuchi, K.; Boeszoermenyi, A.; Hagn, F.; Wagner, G. *J. Biomol. NMR* **2015**, *62*, 291−301. (b) Weininger, U.; Respondek, M.; Akke, M. *J. Biomol. NMR* **2012**, *54*, 9−14.

DOI: 10.1021/jacs.5b07010
J. Am. Chem. Soc. 2015, 137, 11242−11245